

## DETERMINATION OF RTD CURVES FOR ALUMINIUM REFINING PROCESS CONDUCTED IN BATCH REACTOR – PHYSICAL MODELLING

It is really hard to determine the phenomena occurring during aluminum refining process using argon blowing through the liquid metal in industrial conditions. The solution of such problem is physical modelling. This kind of modelling gives possibility to determine the level of dispersion of the refining gas in liquid metal. Especially in steel metallurgy RTD (Residence Time Distribution) analysis and visualization process with some colour tracer, which can give extra information about time of mixing are very popularly used.

Because the modelling research (especially visualization) is pictorial, the research was conducted to check if it is possible to estimate quantitatively impeller working effectiveness basing on determination of the RTD curves. The examined object was model of URO-200 batch refining reactor. The RTD curves was registered and discussed for three different impellers and four different variants of processing parameters (rotary impeller speed: 300-500 rpm, and gas flow rate: 15-20 l·min<sup>-1</sup>). Additionally, the process of mixing of the inert gas with water as a modelling agent was enabled to be observed due to introduction of colour tracer (KMnO<sub>4</sub>). Results obtained from both measuring methods were graphically presented, compared and shortly discussed.

*Keywords:* aluminium refining, barbotage, physical modelling, RTD curves

### 1. Introduction

Physical modelling is today commonly used for finding information about phenomena occurring in many metallurgical reactors – this concerns both iron, steel and non-ferrous metallurgy. Many researchers presents results of modelling process of iron and steel production, from modelling processes occurring in blast furnace [1,2], ladle [3-7], tundish [8-16] and mold [17]. In steel industry typical modelling methods rely on qualitative analysis such as visualization methods using color tracer (such as KMnO<sub>4</sub>) and quantitative analysis such as registration of conductivity changes of NaCl water solution, which is mixed with modelling fluid. Then obtained results are calculated into dimensionless tracer concentration. The last method is used for determination of transient zones and estimation of participation of particular kinds of flow.

Physical modelling becomes more and more popularly used in non-ferrous metallurgy, especially in aluminium refining. There are some publications, which consider refining process conducted in batch [18-23] and continuous reactor [24]. Almost all of the articles focused on the dispersion level of refining gas in the volume of tank with modelling liquid, only in [23] the RTD (Residence Time Distribution) analysis was presented in some detail.

The main aim of the presented research was to determine if the measuring techniques popularly used in steel industry can give correct and full answers considering the effectiveness of impeller work, especially analyzing the technological parameters such as flow rate of refining gas and rotary impeller speed of the particular impeller.

### 2. Research methodology

The water model of the URO-200 batch reactor (made from Plexiglas) for aluminium refining was built in the scale 1:1. The tank of the reactor is transparent to observe phenomena of the mixing process. The model was built according to the theory of similarity using the criterial numbers, which was earlier described in [19]. Fig. 1 shows the scheme of the model of URO-200 refining reactor. Three different impellers were tested, which dimensions and shapes are shown on Fig. 2.

Three sensors (conductometers) were placed in the modelling tank to measure changes of conductivity in different parts of the modelling tank (this place are shown on Fig. 1) with the use of special measuring and controlling apparatus. For such quantitative research the water solution of NaCl was used as a tracer. For visualization method, the KMnO<sub>4</sub> was used as a tracer (its violet

\* SILESIAAN UNIVERSITY OF TECHNOLOGY, FACULTY OF MATERIALS ENGINEERING AND METALLURGY, 8 KRASIŃSKIEGO STR., 40-019 KATOWICE, POLAND,

# Corresponding author: mariola.saternus@polsl.pl

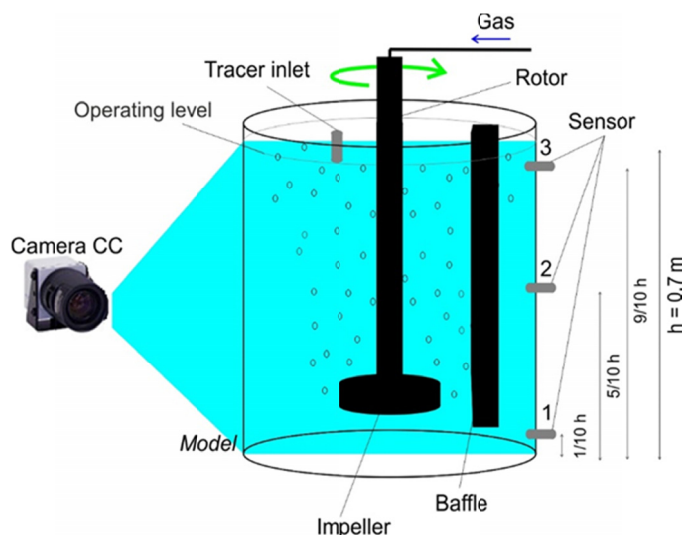


Fig. 1. Scheme of the URO-200 refining reactor model with indication of sensors (conductimeters) places

colour gives the contrast in transparent water). The movement of modelling agent and the mixing phenomena occurring in the model reactor are tested qualitatively registering the course of the experiment by means of high digital camera.

During the research, the main processing parameters such as flow rate of refining gas and rotary impeller speed were changing – Table 1 presents the possible variants of conducted tests for three different impellers.

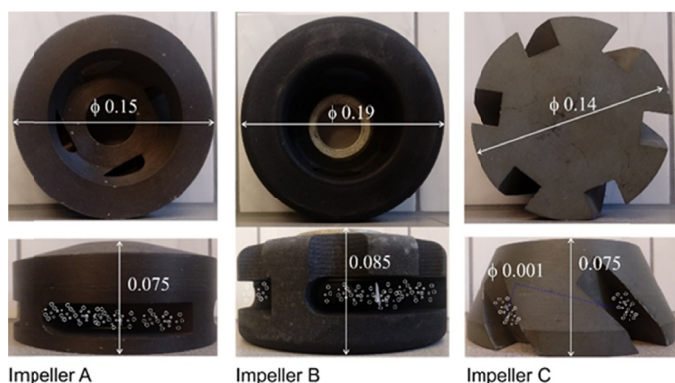


Fig. 2. View of the tested impellers with main dimensions in m

### 3. Results and discussion

During the research the change of conductivity of modelling agent was measured in  $\mu\text{S}\cdot\text{cm}^{-1}$  under the influence of an added tracer in the form of an aqueous NaCl solution. This change was treated as an analog of the change in NaCl concentration in the modelling liquid. If the obtained results can be comparable with each other, the recorded values were calculated to a dimensionless form according to the following formulas [25]:

$$C = \frac{G_{pom}}{G_{max}} \quad (1)$$

TABLE 1

Variants of experimental research for tested impellers

No of var.	Impeller speed, rpm	Gas flow rate, $\text{l}\cdot\text{min}^{-1}$
<b>Impeller A</b>		
A1	300	15
A2	400	15
A3	500	15
A4	400	20
<b>Impeller B</b>		
B1	300	15
B2	400	15
B3	500	15
B4	400	20
<b>Impeller C</b>		
C1	300	15
C2	400	15
C3	500	15
C4	400	20

$$C_b = \frac{c - c_o}{c_\infty - c_o} \quad (2)$$

where:  $C$  – basic dimensionless tracer concentration,  $G_{pom}$  – analog of tracer concentration in time,  $\mu\text{S}\cdot\text{cm}^{-1}$ ,  $G_{max}$  – analog of maximal tracer concentration in modelling liquid,  $\mu\text{S}\cdot\text{cm}^{-1}$ ,  $C_b$  – dimensionless concentration of the tracer,  $C_o$  – base dimensionless concentration of the tracer at the beginning of the process,  $C_\infty$  – base dimensionless concentration of the tracer at the end of the process.

Basing on the results of conducted research, the RTD curves were determined. Figs. 3 to 5 show the dependence of changes in the dimensionless concentration of the tracer in the function of time for chosen variants of experiments for impellers A, B, C. The determined characteristics made it possible to determine the minimum values of mixing times of the tracer in the modelling liquid. The criterion for determining these values was the moment when the concentration of the marker for both measuring points reached a plateau in the range of 0.9-1.1, which means that the tracer was completely mixed in the entire volume of the modelling liquid.

Analyzing RTD curves presented on Figures 3 to 5 it can be observed the big scatter of results in the sensors. However, in the majority cases such curves reached the value 1 (after calculating to the dimensionless concentration). This enables to determine the time of mixing. For impeller A the time of mixing in case of A1 and A2 is more than 40 seconds, for variants A3 and A4 is quicker – about 25 seconds. The time of mixing for impeller B is shorter than for impeller A and it is following for the variants: B1 – 35 s, B2 – 20 s, B3 – 16 s, B4 – 25s. Whereas, the time of mixing in case of impeller C is the following: C1 and C2 – 35 s, C3 – 25 s, C4 – 35s.

Table 2 shows results of the visualization of mixing using  $\text{KMnO}_4$  as a tracer. The view of mixing is presented after 1, 2, 4, 6 and 8 seconds of the process. The results were chosen for variants A1, A3, A4 for impeller A, B1, B3 and B4 for variants B and C1, C3 and C4 for impeller C. Results for variants A2, B2

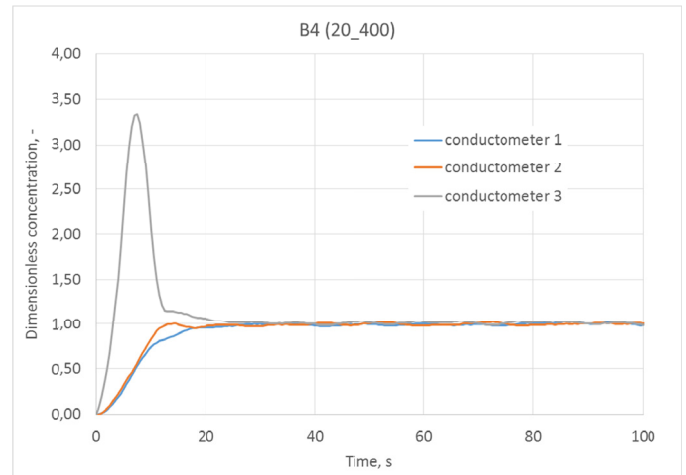
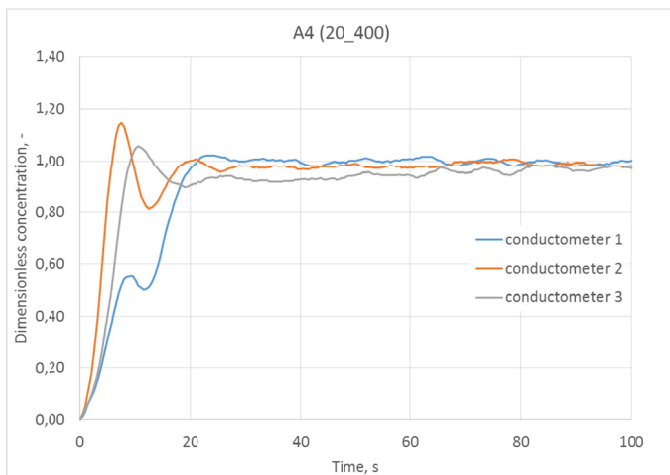
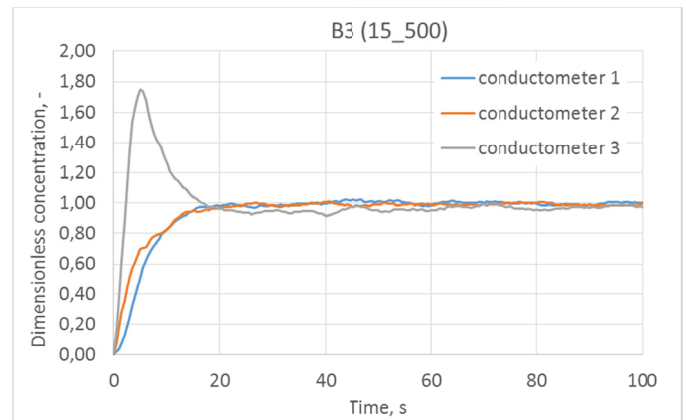
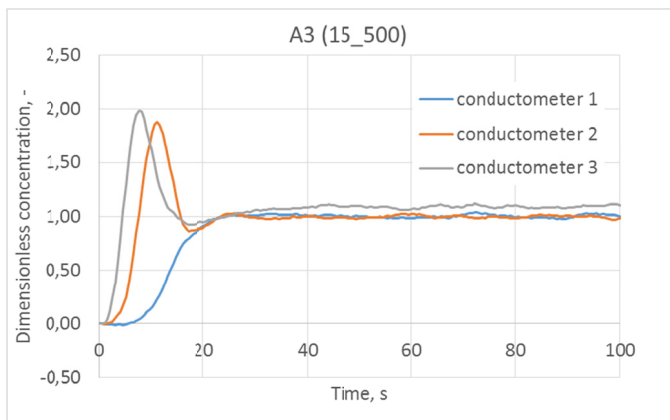
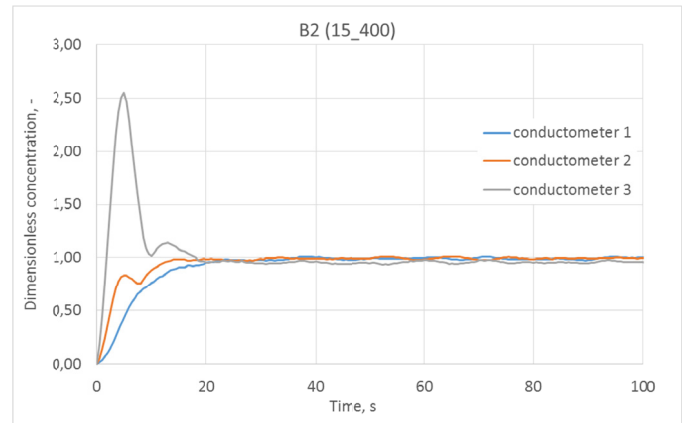
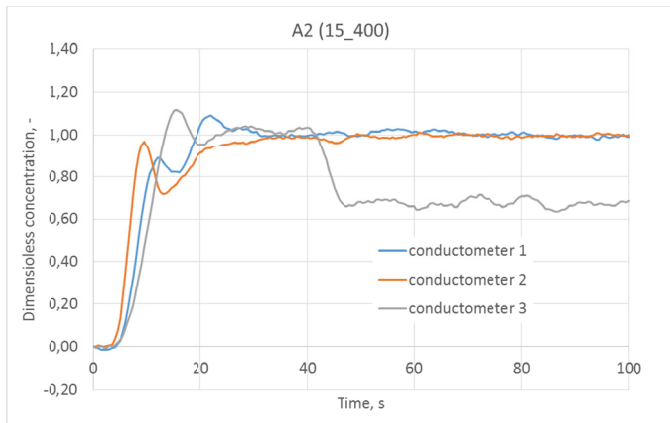
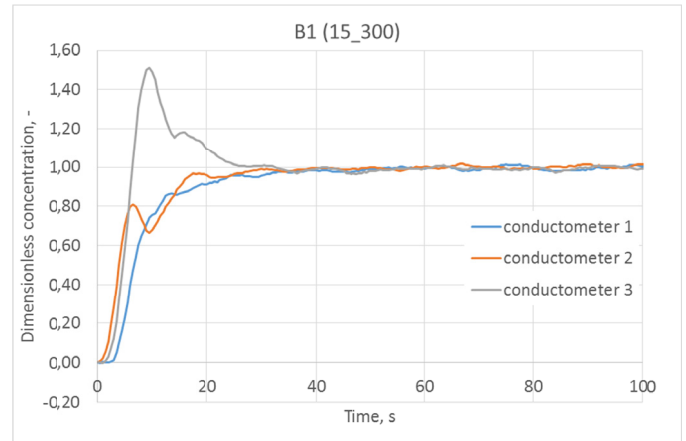
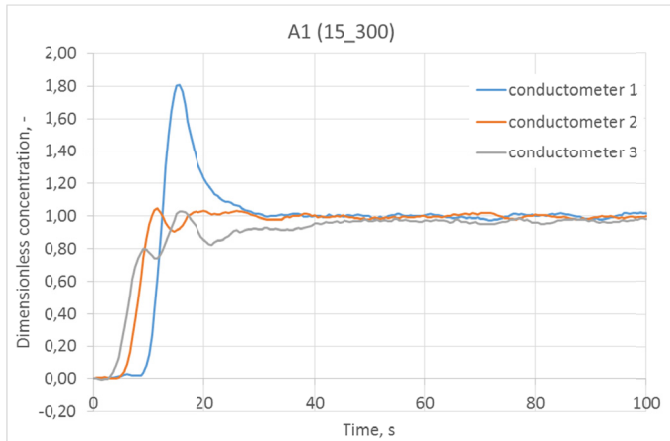


Fig. 3. Determined RTD curves for impeller A – four different variants mentioned in Table 1

Fig. 4. Determined RTD curves for impeller B – four different variants mentioned in Table 1

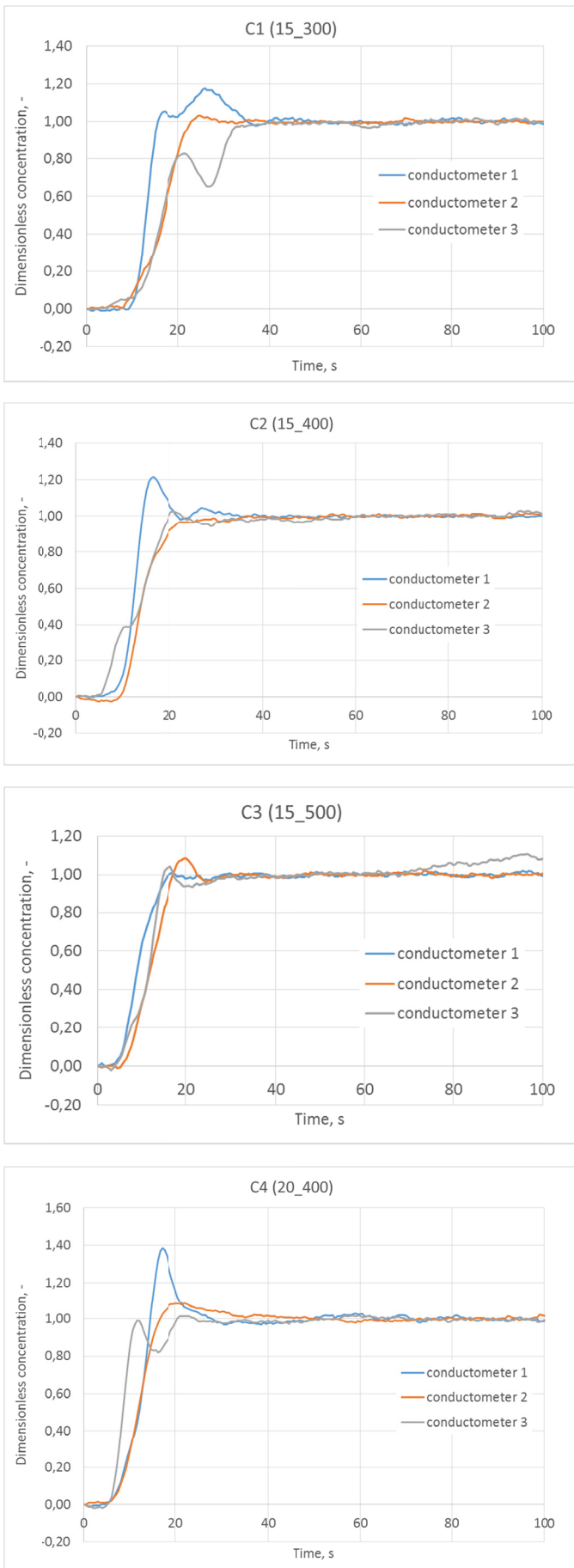


Fig. 5. Determined RTD curves for impeller C – four different variants mentioned in Table 1

and C2 were very similar to variants A1, B1 and C1, so they were skipped. After 8 s only for impeller B (variant B4) the almost full mixing is observed in the whole volume of the modelling tank. The worst result of mixing after 8 s is observed for impeller C. In every cases can be observed dead zones near the baffle, which after 20 s in the worst case disappear.

The results obtained from visualisation are similar to these from RTD analysis. The best impeller seems to be impeller B, however the further research are still needed.

#### 4. Summary and statements

Based on the conducted research, the following conclusions were drawn:

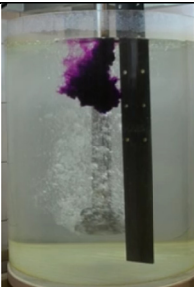









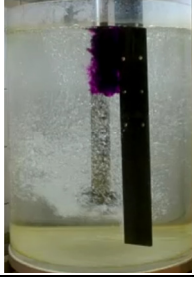
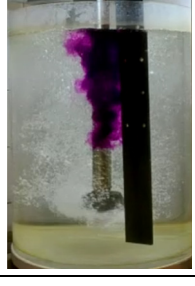



- The results of research indicate that the process of mixing, which is identified by RTD curves, gives the essential knowledge about the identification of important processing parameters of aluminium refining by barbotage (flow rate of refining gas and rotary impeller speed) and their work for particular impeller.
- Results of visualization show that the best parameters for impeller A are  $15 \text{ l} \cdot \text{min}^{-1}$  and 500 rpm (variant A3). The same is in the case of impeller B (variant B3); whereas for impeller C the best processing parameters are  $20 \text{ l} \cdot \text{min}^{-1}$  and 400 rpm (variant C4) or  $15 \text{ l} \cdot \text{min}^{-1}$  and 500 rpm (variant C3). However, it should be also mentioned that the better results of mixing could be obtained when the tracer will be introduced together with the refining gas through the impeller. Unfortunately, it is really hard to conduct, and as a negative results the rotor shaft could be during this process damaged or more susceptible for corrosion.
- From RTD analysis it was observed that the shortest time of mixing was measured for impeller B (variant B3) – 16 seconds, the longest time of mixing was obtained for impeller A (variant A1 and A2) – more than 40 seconds.
- The presented RTD curves do not give clear answer like it is in the process of mixing the alloying elements in the ladle in steel production process, however it enables to estimate properly the technological parameters of reactor work when using the studied impeller. They complemented satisfactorily visualization results of mixing of the tracer in modelling liquid.

The particular answer for the question which impellers is the best working one can confirm research of removing oxygen (simulating hydrogen) from modelling liquid. This kind of research is more expensive, because it needs as a refining gas argon instead of air which is mainly used in visualization process in modelling research. Nevertheless, the mentioned research could complement the results obtained from physical modelling.

TABLE 2

Results of mixing of the  $KMnO_4$  with water – modelling liquid

Probe	Time of mixing of the tracer with the modelling medium, s				
	1s	2s	4s	6s	8s
A1					
A3					
A4					
B1					
B3					
B4					

Probe	Time of mixing of the tracer with the modelling medium, s				
	1s	2s	4s	6s	8s
C1					
C3					
C4					

## REFERENCES

- [1] B. Panic, Archives of Metallurgy and Materials **59**, 2, 795-800 (2014).
- [2] B. Panic, K. Janiszewski, Metalurgija **53**, 3, 331-334 (2014).
- [3] L. Bulkowski, U. Galisz, H. Kania, Z. Kudliński, J. Pieprzycza, J. Barański, Archives of Metallurgy and Materials **57**, 1, 363-369 (2012).
- [4] D. Mazdumdar, R.I.L. Guthrie, ISIJ International **35**, 1-20 (1995).
- [5] K. Michalek, K. Gryc, J. Moravka, Metalurgija **48**, 4, 215-218 (2009).
- [6] D. Guao, G.A. Irons, Metallurgical and Materials Transactions B **31**, 1447-1455 (2010).
- [7] K. Seon-Hyo, R.J. Fruehan, Metallurgical Transactions B **18**, 673-680 (1987).
- [8] A. Kumar, S.C. Koria, D. Mazdumdar, ISIJ International **44**, 8, 1334-1341 (2004).
- [9] K. Chattopadhyay, M. Isac, R.I.L. Guthrie, ISIJ International **50**, 3, 331-348 (2010).
- [10] K. Chattopadhyay, M. Hasan, M. Isac, R.I.L. Guthrie, Metallurgical and Materials Transactions B **41**, 225-233 (2010).
- [11] S. Lopez-Ramirez, J.J. Barretto, J. Palafox-Ramos, R.D. Morales, D. Zacharias, Metallurgical and Materials Transactions B **32**, 7, 615-627 (2001).
- [12] J. Palafox-Ramos, J.J. Barretto, S. Lopez-Ramirez, R.D. Morales, Ironmaking and Steelmaking **28**, 2, 101-109, (2001).
- [13] H. Lei, Metallurgical and Materials Transactions B **46**, 6, 2408-2413 (2015).
- [14] F. Zhang, S. Taniguchi, K. Cai, Metallurgical and Materials Transactions B **31**, 2, 253-266 (2000).
- [15] T. Merder, J. Pieprzycza, M. Saternus, Metalurgija **53**, 2, 155-158 (2014).
- [16] P. Warzecha, M. Warzecha, T. Merder, Metalurgija **54**, 3, 462-464 (2015).
- [17] Y. Kwon, J. Zhang, H-G. Lee, ISIJ International **46**, 2, 257-266 (2006).
- [18] E. Mancilla, W. Cruz-Mendez, I.E. Garduno, C. Gonzalez-Rivera, M.A. Ramirez-Argaze, G. Ascanio, Chemical Engineering Research and Design **118**, 158-169 (2017).
- [19] E. R. Gonzalez, R. Zenit, C. Gonzalez-Rivera, G. Trapaga, M.A. Ramirez-Argaez, Metallurgical and Materials Transactions B **44**, 974-983 (2013).
- [20] J.L. Camacho-Martinez, M.A. Ramirez-Argaez, A. Juarez-Hernandez, C. Gonzalez-Rivera, G. Trapaga-Martinez, Materials and Manufacturing Processes **27**, 556-560 (2012).
- [21] M. Saternus, T. Merder, Metalurgija **54**, 1, 27-30 (2015).
- [22] M. Saternus, Metalurgija **50**, 4, 257-260 (2011).
- [23] M. Saternus, J. Botor, Metalurgija **48**, 175-179, (2009).
- [24] M. Saternus, T. Merder, J. Pieprzycza, Archives of Metallurgy and Materials **60**, 4, 2887-2894 (2015).
- [25] K. Marcinek, J. Pieprzycza, Hutnik **83**, 2, 51-55 (2016).